

Experimental research on the resistojet thruster heater

JAN KINDRACKI*
ŁUKASZ MEŻYK
PRZEMYSŁAW PASZKIEWICZ

Warsaw University of Technology, Institute of Heat Engineering,
Nowowiejska 21/25, 00-665 Warsaw, Poland

Abstract The paper describes experimental research on a resistojet type rocket thruster which was built as an actuator in the Attitude Control System of a model space robotic platform. A key element of the thruster is the heater responsible for increasing the temperature of the working medium in the thruster chamber and hence the specific impulse. This parameter describes the performance of the thruster, increases providing – for lower propellant consumption – the same propulsion effect (thrust). A high performance thruster means either total launch mass can be reduced or satellite lifetime increased, which are key commercial factors. During the first phase of the project, 7 different heating chamber designs were examined. The heater is made of resistive wire with resistivity of $9\Omega/\text{m}$. Power is delivered by a dedicated supply system based on supercapacitors with output voltage regulated in the range of 20–70 V. The experimental phase was followed by designing the chamber geometry and the heating element able to deliver both: maximum increase of gas temperature and minimum construction dimensions. Experiments with the optimal design show an increase in temperature of the working gas (air) by about 300°C giving a 40% increase in specific impulse. The final effect of that is a 40% reduction in mass flow rate while retaining thrust at a nominal level of 1 N.

Keywords: Resistojet thruster; Electric heater; Heat transfer

*Corresponding Author. Email: jkind@itc.pw.edu.pl

1 Introduction

Many space missions require control over the position and orientation of the spacecraft in orbit. They may be used to set spacecraft antennas in the direction of ground stations, solar panels into proper orientation relative to the Sun or sensors and measurement instruments relative to the object of interest. Some missions, especially those on low earth orbit (LEO), require periodic orbital corrections due to the presence of residual atmosphere which negatively influences the altitude of the spacecraft. Moreover, there are a number of disturbances coming from both the environment (external disturbances such as magnetic, gravity, radiation) and from the spacecraft itself (internal disturbances such mechanisms, crew movement, liquid movements) which can perturb the position or orientation of the spacecraft [1]. Required manoeuvres are carried out by the attitude and orbit control system (AOCS), which, depending on the mission requirements, utilizes executive subsystems based on various devices, e.g., reaction wheels, momentum wheels, magnetic actuators and rocket thrusters. One of the most versatile relies on small rocket thrusters [2]. One key parameter of rocket thrusters is a specific impulse, which indicates how much propellant has to be used to produce the unit of thrust in the unit of time [3]. Comparing two thrusters, the one characterized by higher specific impulse consumes lower mass of propellant to produce the same effect – thrust or total impulse. There are plenty of types of thrusters which are used by attitude and orbit control systems. Increasing interest in low-cost missions performed by small to mid size satellites, e.g., for Earth observation [4–6] and robotic platforms [7] is driving the continuous improvement in thruster parameters. The highest specific impulse at present is delivered by the ion engine, but maximum thrust in the region of 250 mN [8] limits its application to missions which do not require highly dynamic maneuvers. On the other hand, while chemical thrusters can operate across a very wide range of thrust, their application can be limited by the toxicity of the propellants and their potentially harmful influence on on-board apparatus, sensitive to pollution coming from the products of combustion, e.g., telescope mirrors. For the class of mission with required thrust of 0.1–1 N, non-chemical, electrothermal thrusters of the resistojet type can be considered as a solution.

Resistojet has the simplest construction in the electrical rocket thrusters family. Its principle of operation is common with chemical thrusters – thrust is a reaction force harnessing high velocity expulsion of gaseous products from the nozzle. The characteristic feature for the resistojet thruster

is the manner of increasing medium energy inside the chamber. Chemical thrusters utilize the chemical energy stored in the propellant and released during the process of combustion or decomposition [9]. In the resistojet thruster, energy is stored in the gas as potential energy of pressurized medium and in electrical power supply to the gas. The electrical energy is transferred to the gas by a heated element which has direct contact with the flowing medium [10]. The heating process increases the parameters (specific impulse) of the engine in contrast to the cold gas system, which simply expands the cold medium directly from the feeding system using the de Laval nozzle [11]. This is important as regards propellant consumption. Additionally, the heating chamber may also be used as an evaporator for liquid propellants which are characterized by higher density and so the volumetric specific impulse – the one referred to the volume of the propulsion system [12]. The crucial element of the resistojet thruster is the heating element, which is also the part most susceptible to wear and tear.

The challenge is to develop the heating element – and organize the medium flow around it – to obtain maximum heat transfer and gas temperature together with a long lifetime of up to several thousand cycles, depending on mission requirements. It should be clear for the reader that the increase in specific impulse causes an increase in power demands for heating and hence power supply mass and volume. There is an optimum value above which increasing the specific impulse of the electric thruster is unprofitable due to the disproportionate increase in power supply mass [13]. Most current resistojets generate thrust of 20–300 mN [14], but using new, efficient power sources, e.g., based on supercapacitors, opens the way to raising the thrust to about 1 N. When drawing up the propulsion system for the model robotic platform, authors designed and developed resistojet thrusters with nominal thrust of 1 N fed by nitrogen gas as propellant. In this paper the authors describe the development and laboratory research on various concepts of the resistive heater as a main element of the resistojet, performed during the initial stage of the project.

2 Research stand

The research stand consists of a few key elements: gas feeding system, thruster chamber with heating element (the chamber ends with a critical nozzle diameter), electrical power supply system and measurement system. The gas feed system consists of a pressure accumulator connected to an

external gas source, a pressure regulator to set the working pressure, feeding lines, a Venturi orifice and an electromagnetic valve for flow control. An overview of the stand is shown in Fig. 1. Air is used as a working

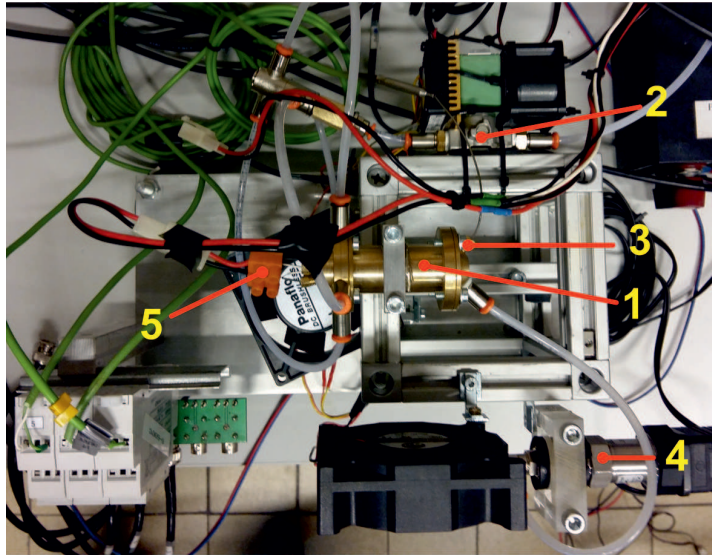


Figure 1: General view of the research stand: 1 – heating chamber, 2 – electromagnetic valve, 3 – thermocouple to measure the gas temperature at the heater outlet (about 1% accuracy – depended on the measurement temperature range), 4 – pressure transducer (0.2% full scale accuracy), 5 – heater electrical connectors.

medium. Although it is rarely used in propulsion system applications, the performance parameters and thermodynamic properties are very close to nitrogen, the nominal propellant. The decision to use air was driven by pragmatic concerns: the possibility of connecting the stand to an external source of compressed air supplied by a compressor, which means steady inlet parameters can be easily maintained unchanged for a long time. Opting to use air as a medium was of course cheaper: a very important consideration when preparing long-term experiments. To compensate for pressure fluctuations on the feeding line a 0.029 m³ tank was used as a pressure accumulator. The working pressure was set by a high precision pressure regulator: Tescom model BB13AL3KVA4. An in-house modified Parker valve was used as the main control valve. The valve modifications were proved in a developed model of the cold gas system described in [11]. After modification, the valve can operate with an opening time of 3.5 ms and frequency of 35 Hz.

The main element of the stand is a heating chamber ending with a critical nozzle diameter, which was the object of investigation. The task for this stage of the project was to find the most advantageous chamber geometry to maximize the thermal energy transfer between the heater and flowing gas. The research included 5 various geometries in different configurations, as presented in Fig. 2.

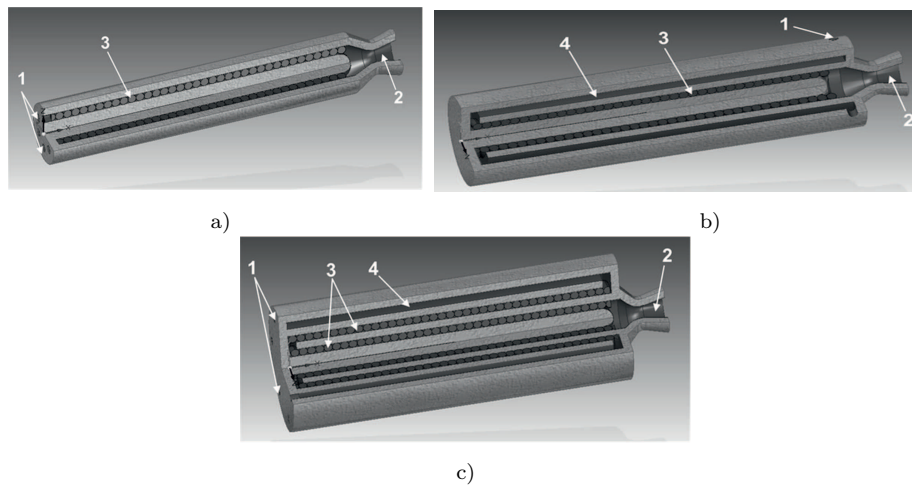


Figure 2: Schematic diagrams of the investigated heating chamber of the resistojet thruster - a) geometry C1, b) geometries C4 and C4a, c) geometries C2, C3, C5a and C5b: 1 – gas inlet, 2 – nozzle, 3 – heating channel, 4 – energy recovery channel.

The divergent part of the nozzle was not used, because it was not necessary for the heat transfer investigation. Additionally, the problematic manufacturing process for such small geometries would increase the costs of the research unnecessarily. A critical cross-section of the nozzle was sufficient to maintain the assumed pressure inside the chamber for all geometries and was relatively easy to manufacture. The heater inside the chamber was made of resistive wire with a diameter of 0.3 mm covered by insulator and enclosed in a stainless steel coat. The external diameter of the heating wire is 1 mm (with insulator and external coating) and the resistivity at room temperature is 9 W/m. Using the wire provides a high level of flexibility in terms of heater formation – the only limitations are fillet radius and wire length due to the required value of resistance. During the research one or two heaters connected in series or parallel were investigated. When

using two heaters of different diameter, two configurations were possible: the same wire length or the same number of coils. For the same number of coils the external and internal heaters have different wire length and so the resistance. It is an adverse effect because of different thermal loads for both heaters: one of them is under loaded, which generates losses. In the other case, when the wires have the same length, both are similarly loaded but the distance between the coils is greater for the external heater, which generates losses due to the cooling of the flow between the successive coils. As presented in Fig. 2 and Tab. 1, all configurations except C1 have an additional external channel without a heater. The medium flowing through that empty channel partially recovers the heat which would normally be radiated to the environment, increasing losses. Introducing a third channel improves the efficiency of heating the gas inside the chamber.

Table 1: Description of various geometries and connections investigated in the laboratory.

No.	Description	Number of heated channels	Number of un-heated channels	Single channel length [mm]	Voltage range [V]	Power range [W]
C1	Single channel construction (material: stainless steel)	1	0	40	30–45	140–320
C2	Three channels, heaters connected in parallel, similar heater length	2	1	40	30–40	240–430
C3	Three channels, heaters connected in parallel, similar resistance of heaters	2	1	40	30–45	360–640
C4	Two channels – only one heated	1	1	20	25–32.5	210–350
C4a	Two channels, one heated, external wall of the heating channel made of ceramic material	1	1	20	20–30	275
C5a	Three channels, heaters connected in parallel	2	1	20	20–30	250–550
C5b	Three channels, heaters connected serially	2	1	20	50–60	350–600

The power source for the heaters, in this stage of the project, is based on one or two direct current laboratory power supplies with regulated voltage

(0–60 V) and current (0–10 A) levels. The choice of source depends on the requirements. They work as a constant voltage source and the power delivered is regulated by the flowing current, which varies slightly due to the changes in heater resistance with changing temperature. The heater control system which sets the start of heater work and its time of operation is based on a solid state relay (SSR) switch connected directly to the data acquisition and control system (DAQ) – a PC computer with in-house software – giving precise control over the heating process.

3 Experiments

The experimental setup was the same for all geometries. The pressure regulator was set to obtain 1 MPa of operating pressure inside the chamber. For various experiments the voltage setting was chosen from the range 20–45 V with the exception of some experiments when the heaters were serially connected, increasing the total resistance. That gives an opportunity to increase the voltage up to 60 V. A higher voltage level was preferred due to the planned power system based on supercapacitors with a maximum voltage level of 70 V for the final construction. The total power of the heater was 640 W, which gives over 10 A of current when setting the source at a voltage of 60 V. The value of 10 A is a limitation for the wire, which creates a risk that the heater may fail in the case of a temporary severe reduction or absence of flow. Using DAQ software the delay between opening the valve and starting the heater was set in the range of 0–4 s. For most of the experiments the time period of heater operation was set at 20 s as compared to 50 s of gas flow. The additional 30 s was used to cool the elements of the thruster to the initial temperature between the experiments, thereby increasing the level of repeatability. Experiments for every set of settings (parameters of the research stand) were repeated at least 10 times, to reject outlier results and still obtain mean values of the parameters based on a significant number of experiments. The relatively long duration of experiments enabled the quasi-steady conditions (e.g. temperature) inside the chamber to be established, which gave an opportunity to compare different configurations. Figure 3 illustrates the exemplary time course of parameters measured during a single experiment. In this case, the valve-heater delay was set at 0 s. A relatively slow heating process occurred – a long time was required to establish the quasi-steady conditions – which is visible on the temperature graph. This is also confirmed by the Venturi pressure

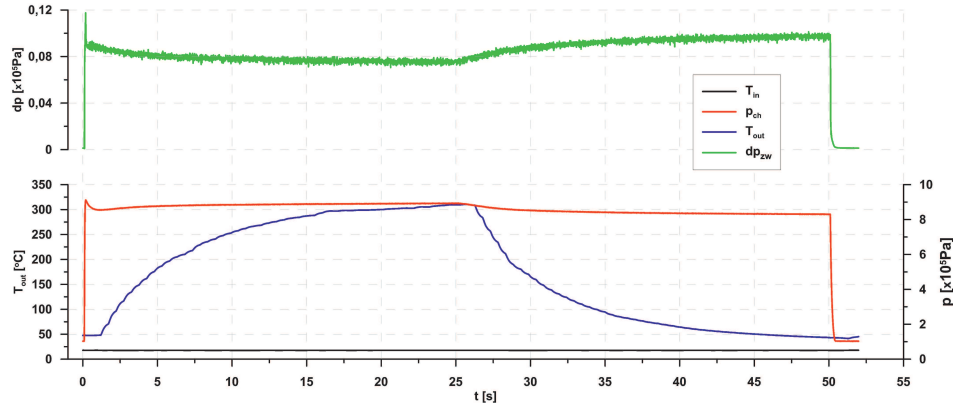


Figure 3: Exemplary time course of parameters measured during experiments.

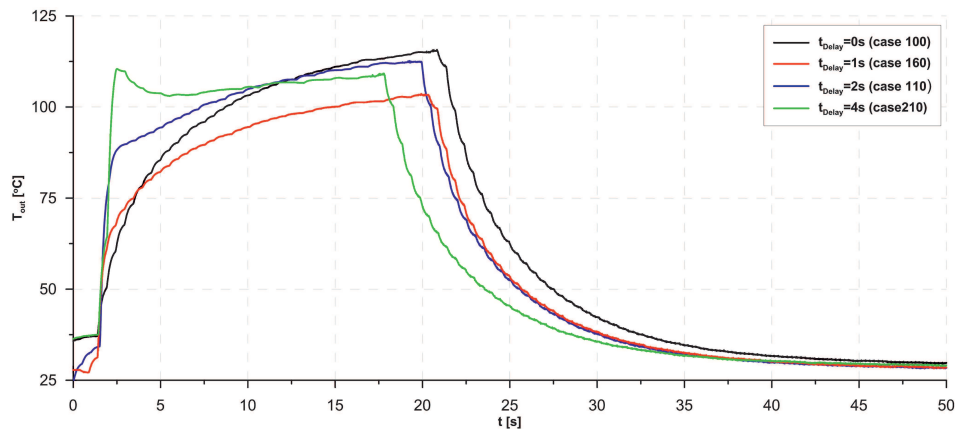


Figure 4: Influence of the heater-valve time delay on the rate of gas temperature increase at the outlet area of the chamber for geometry C1.

drop, which is caused by the decrease in mass flow rate along with the rising temperature of the gas. Figure 4 presents the influence of the time delay between starting the heater and opening the valve on the rate of gas temperature increase at the outlet area of the chamber. It can be clearly seen that the time delay of 2 s causes a significantly higher heating rate than the 0 s delay. It should be borne in mind that temperature cannot be translated directly into a conclusion on the thruster dynamics due to the high thermocouple inertia, which depends on the size and design of the temperature sensor. Figure 5 shows the influence of the power level on the

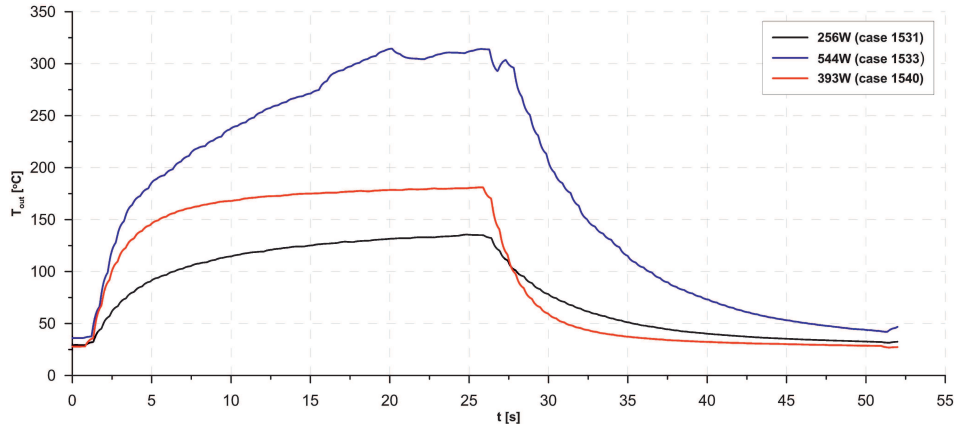


Figure 5: Influence of the power delivered to the heater on the gas temperature at the heater outlet area for the geometry C5a.

gas temperature at the outlet area for the same pressure inside the chamber and heater-valve delay time.

4 Results analysis

During research into the optimal heater, five basic geometries with additional variants were investigated. As mentioned in the previous section, Tab. 1 presents the parameters and settings for all analyzed geometries described below. To compare the heating effectiveness for various geometries an appropriate indicator has to be chosen. For the purpose of this work a new coefficient, independent of geometry was designed, called the ‘power requirement coefficient’. It may be calculated as a ratio of heater power to gas temperature at the outlet and mass flow rate. It gives information on the power required to heat up unit flow by one degree. In brief: the lower the coefficient, the higher the heater efficiency. Figure 6 presents a comparison of the power requirement coefficient for the geometries described in Tab. 1. Looking at the results, geometry C5 may be described as the most efficient, regardless of the heater connection type (serial or parallel). The values of the coefficient obtained are in the range of 1000–1700 W/°C kg/s. Such a wide range is caused by putting all the data (for different voltage levels and heater-valve delay times) on a single graph. In the case of C1 geometry a rapid drop in the coefficient can be seen for the experiments with numbers between 650 and 820. For those experiments the heater was

replaced due to damage to the first one caused by overheating during the research campaign. Due to the technical difficulties involved in keeping similar a length of wire, the new heater had different parameters – which created inconsistency in the results obtained during the second part of the campaign. This demonstrates just how important the geometry of a heater is for the repeatability of results. In Fig. 7 the power requirement parameter as a function of voltage level for a heater-delay time set at zero is presented. This confirms how important heater geometry is for repeatability, i.e., the number of coils, the diameter and the length of wire.

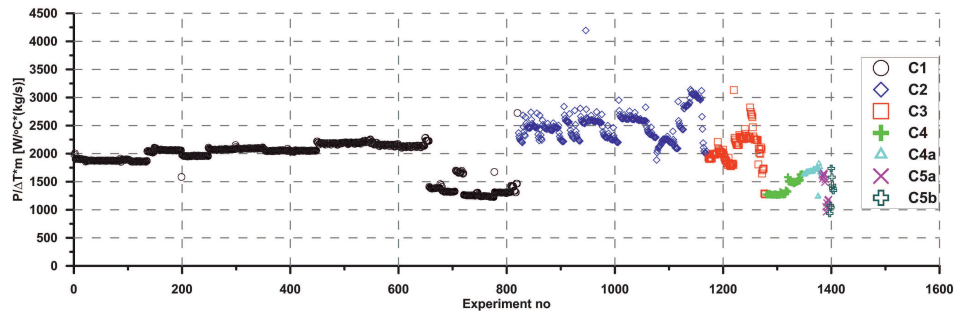


Figure 6: Power requirement coefficient for investigated geometries.

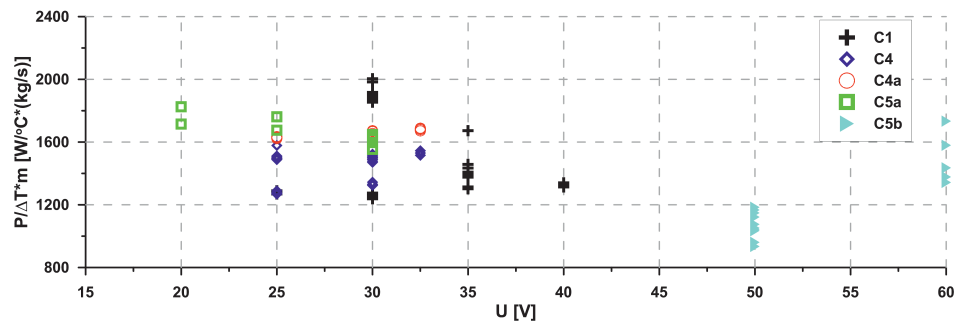


Figure 7: Power requirement coefficient as a function of applied voltage for investigated geometries (heater-valve delay time was set at 0 s).

The pressure drop between the inlet and outlet of the heating chamber is another important comparative parameter for the various geometries. The pressure drop measurements for all investigated geometries are presented in Fig. 8. The highest pressure drops of 6–9% were measured for geometries C1 and C4. Geometries C2 and C3 delivered the lowest losses of 2–3%. Ge-

ometry C5, the most efficient geometry according to the power requirement coefficient, is characterized by intermediate losses of 5%. When seeking to maximize the efficiency of heat transfer two factors have to be considered – velocity of flow and turbulence level. Very low velocity of flow results in large losses to the external walls of the chamber. On the other hand, high velocity shortens the gas residence time in the chamber so it does not have time to heat up properly. The flow should be organized in a way which assures an intermediate velocity of flow together with a fine level of turbulence, which mixes the flow – increasing the heat transfer coefficient – and unifies the temperature at the outlet area. To limit the losses to the ambient at least the external walls of the chamber should be made of materials which restrict heat transfer, e.g., with ceramic coatings. Another way is to organize the flow around the walls before it enters the heating chamber and so restore some energy from the wall. Using both methods at once might be a perfect solution, but it complicates the design of the heating chamber. Also, an overly long residence time may significantly lower the dynamics of the system. Optimal choice of heating chamber parameters – length, gas velocity, pressure losses – is not a trivial matter and should be predicted by extended investigation.

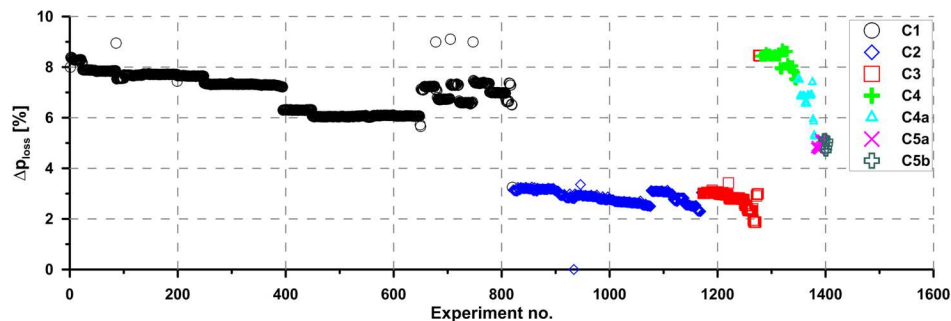


Figure 8: Pressure losses generated by the heater depends on the construction.

Efficiency of heat transfer, as mentioned before, may be described as a ratio of real temperature increase to theoretical increase. This efficiency was defined as a ratio between electrical energy delivered to the heater and increasing of the working gas energy, measured as the gas temperature change. When calculating the energy, the value of specific heat for air was set at 1000 J/kg K and, for simplicity, this was assumed as the constant value regardless of the air temperature. Figure 9 shows the heating efficien-

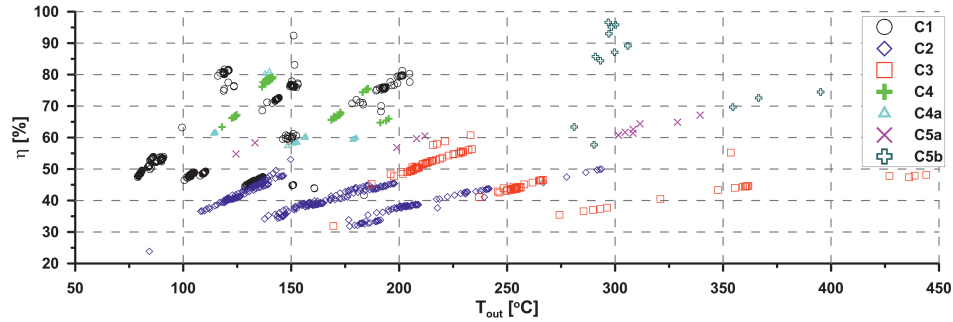


Figure 9: Gas heating efficiency as a function of outlet temperature for the investigated geometries.

cies obtained for all investigated cases using this simple approach. For all considered geometries there are a few groups of values, which are caused by putting the data for several voltage levels and heater-valve delay times on a single graph. The influence of voltage level is presented in Fig. 10a, and heater-delay time in Fig. 10b for the single geometry C1 as an example. Geometry C5 with serially connected heaters delivers maximum efficiency. This connection causes the same current in both heaters and so in the heating power released. It increases efficiency and again reveals the superiority of C5 geometry over the others.

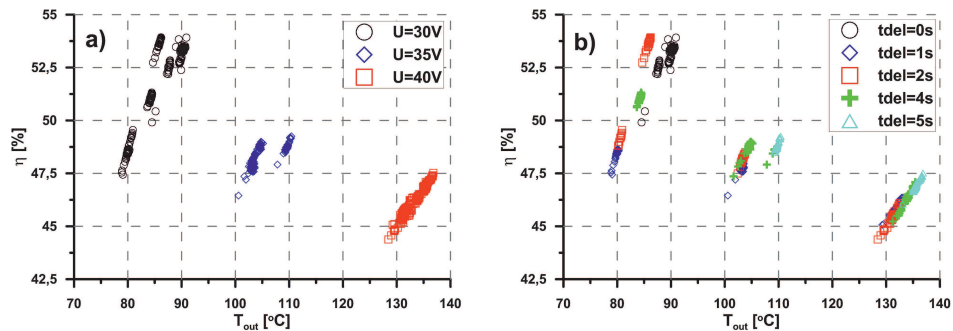


Figure 10: Gas heating efficiency as a function of outlet temperature for geometry C1: a) for different voltage levels; b) for different heater-valve time delays.

Mass flow rate as a function of temperature (Fig. 11) is also in line with expectations – it decreases with rising temperature and for C5 geometry is about 1.22 g/s. Different mass flow rates for various geometries may be explained by the fact that the critical diameters in the models were

manufactured with limited accuracy. Additionally, as was shown before, the various geometries have different pressure drops in the heating chambers, which also influences the mass flow rate for every geometry.

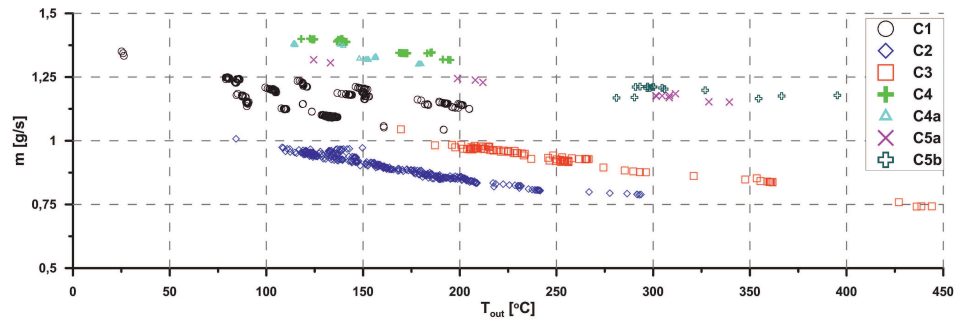


Figure 11: Influence of the outlet temperature on the mass flow rate for various geometries.

5 Summary and conclusions

The research is concentrated on investigating the most important element of the resistojet thruster – the electric heater. It is a key element, because its efficiency contributes greatly to the effectiveness of the thruster. Additionally, the mass, volume and geometry influence the level of complication of the engine. This paper presents various geometries, with one, two or three channels together with various configurations of heaters. Geometries with two heaters are more complicated but substantially increase the power delivered to the gas. A useful option can be added in the form of heater connection types: serial or parallel. Using geometries with an additional channel without a heater, again, complicates the geometry but losses to the environment are limited and increase the efficiency of the system.

At the final stage of the investigation seven various geometries were developed, differing from each other as regards the number of channels, number of heaters and their length. Finally, the most efficient geometry – with three channels and two heaters – was determined based on the developed power requirement coefficient. Geometries C5a and C5b, with heaters of 0.2 m in length, require about 1000–1700 W/(K kg/s) which may be translated into 1.7 W/K for the required mass flow rate. This value also depends on the delay time between the start of heating and opening the valve (heater-valve delay time). Sufficient effects – an increase of thruster

dynamics – are noticeable for a delay time of 1.5 s. Any further increase in delay time leads to reduced flexibility of engine operation.

Pressure drop measurements reveal a maximum loss of 9% of pressure with the value of 5% for the finally chosen geometry, as a satisfactory value. The mass flow rate of the working medium decreases as the gas temperature increases, so thrust is independent of chamber temperature. Heat transfer efficiency is identified as the ratio of energy of the working medium after the heating process (based on temperature measurements) to the energy of the current delivered to the heaters. The values lie within rather wide borders of between 35% and 90%, mainly dependent on the geometry. The total heat transfer efficiency includes the internal efficiency of the heater and the efficiency of the heater-gas heat transfer. Efficiency increases with rising temperature for the investigated cases. It is 70–80% for the chosen geometry in laboratory conditions.

Summarizing, the research has produced valuable data for teams seeking to determine the optimal geometry of the heating element for a low thrust resistojet engine, taking into account required energy, geometrical dimensions together with analysis of the manufacturing possibilities and costs. The next step is to build a model resistojet made of 316L stainless steel and to re-evaluate its effectiveness, together with mass flow rate and thrust measurements. It will lend added insight into propulsion parameters such as specific impulse and energy balance, allowing the system to be compared with others, such as cold gas. Moreover, it will help deliver an answer to the issue of what level of complication would be justified by increased parameters in the context of increased costs and additional power requirements.

Acknowledgments This research was conducted in the framework of the Applied Research Program project, financed by the National Centre for Research and Development, Poland PBS3/A3/22/2015.

Received 28 November 2017

References

- [1] FORTESCUE P.W., STARK J., SWINERD G.: *Spacecraft Systems Engineering*. Wiley, New York 2003.
- [2] LEY W., WITTMANN K. AND HALLMANN W.: *Handbook of Space Technology*. American Institute of Aeronautics and Astronautics, Washington, DC 2009.

- [3] SUTTON G.P. AND BIBLARZ O.: *Rocket Propulsion Elements*. Wiley, New York 2010.
- [4] FOUQUET M., SWEETING M.: *UoSAT-12 Minisatellite for high performance earth observation at low cost*. *Acta Astronaut.* **41**(1997), 3, 173–182, [https://doi.org/10.1016/S0094-5765\(97\)00181-1](https://doi.org/10.1016/S0094-5765(97)00181-1)
- [5] TYC G., TULIP J., SCHULTEN D., KRISCHKE M., OXFORD M.: *The RapidEye mission design*. *Acta Astronaut.* **56**(2005), 1–2, 213–219, <https://doi.org/10.1016/j.actaastro.2004.09.029>
- [6] DA SILVA CURIEL A., BOLAND L., COOKSLEY J., BEKHTI M., STEPHENS P., SUN W., SWEETING M.: *First results from the disaster monitoring constellation (DMC)*. *Acta Astronaut.* **56**(2005), 1–2, 261–271, <https://doi.org/10.1016/j.actaastro.2004.09.026>
- [7] FLORES-ABAD A., MA O., PHAM K., ULRICH S.: *A review of space robotics technologies for on-orbit servicing*. *Prog. Aerosp. Sci.* **68**(2014), 1–26, <https://doi.org/10.1016/j.paerosci.2014.03.002>
- [8] SHIGA D.: *Next-generation ion engine sets new thrust record*. Daily news, 28 September 2007, <https://www.newscientist.com/article/dn12709-next-generation-ion-engine-sets-new-thrust-record/> (accessed 24 Apr. 2017).
- [9] SFORZA P.M.: *Theory of Aerospace Propulsion*. A volume in Aerospace Engineering, Butterworth-Heinemann, 2012.
- [10] JAHN R.G.: *Physics of electric propulsion*. Dover Publications, 2006.
- [11] KINDRACKI J., TUR K., PASZKIEWICZ P., MEŻYK Ł., BORUC Ł., WOLAŃSKI P.: *Experimental research on low-cost cold gas propulsion for a space robot platform*. *Aerosp. Sci. Technol.* **62**(2017), 148–157, <http://dx.doi.org/10.1016/j.ast.2016.12.001>
- [12] GIBBON D., BAKER A., COXHILL I., SWEETING S.M.: *The Development of a Family of Resistojet Thruster Propulsion Systems for Small Spacecraft*. In: Proc. 17th Ann. AIAA/USU Conf. on Small Satellites, SSC03-IV-8, 14 Aug. 2013.
- [13] *What, when, how Portal: Rockets, Ion Propulsion*. <http://what-when-how.com/space-science-and-technology/rockets-ion-propulsion/> (accessed: 28.04.2017).
- [14] ARCIS N., BULIT A., GOLLOR M., LIONNET P., TREUET J.C., GOMEZ I.A.: *Report D2. 1 Database on EP (and EP-related) technologies and TRL*. Rep. EPIC-CNES-2.1-RP-D2.1-1.2 (2015).